J. Fluid Mech. (1996), *vol.* 322, *pp.* 201–214

Forced convection in a fluid-saturated porous-medium channel with isothermal or isoflux boundaries

By D. A. NIELD[1], S. L. M. JUNQUEIRA[2] AND J. L. LAGE[2]

[1] Department of Engineering Science, University of Auckland, Auckland, New Zealand

[2] Mechanical Engineering Department, Southern Methodist University, Dallas, TX 75275–0337, USA

(Received 9 August 1995 and in revised form 14 March 1996)

We present a fresh theoretical analysis of fully developed forced convection in a fluid-saturated porous-medium channel bounded by parallel plates, with imposed uniform heat flux or isothermal condition at the plates. As a preliminary step, we obtain an 'exact' solution of the Brinkman–Forchheimer extension of Darcy's momentum equation for flow in the channel. This uniformly valid solution permits a unified treatment of forced convection heat transfer, provides the means for a deeper explanation of the physical phenomena, and also leads to results which are valid for highly porous materials of current practical importance.

1. Introduction

Because of its relevance to a variety of situations (e.g. geothermal systems, thermal insulation, coal and grain storage, solid matrix heat exchangers, nuclear waste disposal), convection in porous media is a well-developed field of investigation. The literature on the topic of forced convection is surveyed in chapter 4 of Nield & Bejan (1992).

Studies on forced convection in a channel progressed chronologically towards complex models. The groundbreaking study by Kaviany (1985) presented an analytical solution of the transport equations based on the Brinkman-extended Darcy flow model. An important step towards predicting transport phenomena in more general and complex situations was taken by Vafai & Kim (1989), who presented a closed form solution of the Brinkman–Forchheimer-extended Darcy momentum equation and the associated heat transfer equation for the case of fully developed flow with uniform heat flux at the boundaries. The analysis was limited to the case of effective viscosity equal to fluid viscosity. (It is true that one can extend their solution to an effective viscosity model; this involves redefining their Darcy number and inertia parameter.) Vafai & Kim assumed a boundary-layer-type developed flow and as a consequence their solution is inaccurate when the inertia parameter is small and the Darcy number approaches and exceeds the value unity. In the absence of an accurate general theoretical solution one has to rely on direct numerical simulation. Noteworthy in this line are the numerical (and experimental) studies by Poulikakos & Renken (1987) and Renken & Poulikakos (1988), who employed a finite-difference formulation of the differential equations. These authors allowed for viscosity variations, and they were able to deal with developing flow and to incorporate expressions for the permeability and Forchheimer coefficient pertinent for packed beds of spheres, and they performed

calculations for parameter values appropriate for their experiments. Renken & Poulikakos found a substantial degree of agreement between their observations and their predictions, but they were limited to a special type of medium and to a comparatively limited range of parameters, so it is not obvious how far their work generalizes to other porous media.

Although the majority of existing porous materials do satisfy the implicit restrictions inherent in Vafai and Kim's solution, there are at least three practical examples of materials with high permeabilities that do not. The first is an aluminium alloy porous foam for building a microporous heat sink. This device, being developed jointly by Lage's research group at Southern Methodist University and Texas Instruments Inc., is designed for cooling the next generation of high-power electronic components (Lage *et al.* 1996). Preliminary laboratory tests (Weinert & Lage 1994) indicate permeabilities of compressed foams as high as $8 \times 10^{-6}\,\mathrm{m}^2$. For a 1 mm thick foam layer, the equivalent Darcy number is equal to 8. Another example of high permeability material is provided by a resorbable microporous intravascular stent for gene therapy applications (Rajasubramanian *et al.* 1994). This biocompatible material, based on a blend of poly-lactic acid and poly-caprolactone, is being developed at the Southwestern Medical Center at Dallas. Finally, the recent work by Givler & Altobelli (1994) demonstrated that for high-permeability foam the effective viscosity is about 10 times the fluid viscosity. Therefore, a theoretical solution that is general enough to yield accurate results even for highly permeable media is of fundamental and practical interest. This is the object of the present paper. (It extends the results reported by Nakayama, Koyama & Kuwahara (1988) to include the effects of quadratic drag (the Forchheimer extension).)

We reconsider the analysis presented by Vafai & Kim (1989) without invoking their boundary-layer assumption. We then proceed to find a more general theoretical solution. Such a solution has the advantage that the way in which inertial and boundary-friction effects affect the velocity and temperature profiles, and the Nusselt number, can be readily unravelled, for a general porous medium. Furthermore, this solution serves as a benchmark for assessing numerical schemes simulating more complex transport phenomena within high-permeability media. Our solution is based on scaling which avoids the use for this purpose of the mid-line velocity (which cannot be related theoretically to the applied pressure gradient until the solution has been calculated), and this is an obvious practical advantage in the laboratory situation.

2. Isoflux surfaces: theory

We start by making a fresh scaling of the steady-state momentum and energy equations, for one dimensional motion, namely

$$\tilde{\mu}\frac{\mathrm{d}^2u^*}{\mathrm{d}y^{*2}} - \frac{\mu}{K}u^* - c_F\rho K^{-1/2}u^{*2} + G = 0, \tag{1}$$

$$u^*\frac{\partial T^*}{\partial x^*} = \kappa_m\frac{\partial^2 T^*}{\mathrm{d}y^{*2}}. \tag{2}$$

The notation largely follows that used by Nield & Bejan (1992) where K is the permeability, c_F is the inertial coefficient, ρ is the fluid density, and κ_m is the effective thermal diffusivity of the saturated porous medium. The asterisks denote dimensional variables. We assume that we have flow in the positive x-direction (Darcy velocity,

$u^*(y^*) > 0$) resulting from a constant applied pressure gradient $G = -\mathrm{d}p/\mathrm{d}x$. An effective viscosity $\tilde{\mu}$ is introduced in the Brinkman term. The axial component of heat conduction is neglected; this is justified if a Péclet number (based on the channel width as lengthscale) for the flow is sufficiently large. Isotropy, homogeneity, and local thermodynamic equilibrium are assumed.

The effect of thermal dispersion was not considered by Vafai & Kim (1989) nor by Poulikakos & Renken (1987), and neither is it included in the present analysis. We know of no reason why this effect should alter our conclusions dramatically. The effect certainly does not affect the exact fully-developed velocity profile. The transverse dispersion may be taken into account by increasing the thermal diffusivity by a percentage which is of order of magnitude equal to a Péclet number based on the particle diameter as lengthscale. For the fully developed flow treated in this paper, the effect of longitudinal dispersion is not expected to be important in normal situations, but, as was emphasized by a referee, there are situations where the effect is likely to be important.

The flow, as shown in figure 1, is between infinite horizontal plates at $y = H$ and $y = -H$ and a uniform heat flux q'' (into the porous medium) is imposed at each plate. The flow is symmetrical about the midplane, and so the boundary conditions are

$$u^* = 0, \quad \frac{\partial T^*}{\partial y^*} = \frac{q''}{k} \quad \text{at} \quad y^* = H, \tag{3}$$

$$\frac{\partial u^*}{\partial y^*} = 0, \quad \frac{\partial T^*}{\partial y^*} = 0 \quad \text{at} \quad y^* = 0, \tag{4}$$

where k is porous medium thermal conductivity, and q'' is constant. We introduce non-dimensional variables defined by

$$y = \frac{y^*}{H}, \quad u = \frac{\mu u^*}{GH^2}, \tag{5}$$

and the non-dimensional numbers

$$M = \frac{\tilde{\mu}}{\mu}, \quad Da = \frac{K}{H^2}, \quad F = \frac{c_F \rho G H^4}{K^{1/2}\mu^2}. \tag{6}$$

Thus, M is a viscosity ratio, Da is a Darcy number, and we may refer to F as a Forchheimer number.

In non-dimensional form, equation (1) becomes

$$M\frac{\mathrm{d}^2u}{\mathrm{d}y^2} - \frac{u}{Da} - Fu^2 + 1 = 0. \tag{7}$$

This equation can be integrated to give: $M(\mathrm{d}u/\mathrm{d}y)^2 - u^2/Da - \frac{2}{3}Fu^3 + 2u = C$, where C is a constant. This can be written in the form

$$\frac{\mathrm{d}u}{\mathrm{d}y} = -(2F/3M)^{1/2}[P(u)]^{1/2}, \tag{8}$$

where the cubic polynomial $P(u) = (u-b_1)(u-b_2)(u-b_3)$, where the roots b_1, b_2, b_3 are constants satisfying $b_1 < b_2 < b_3$ and $b_2 = u(0)$. This is consistent with the boundary condition (4), and the requirement that $\mathrm{d}u/\mathrm{d}y$ be real and negative when $0 < u < u(0)$.

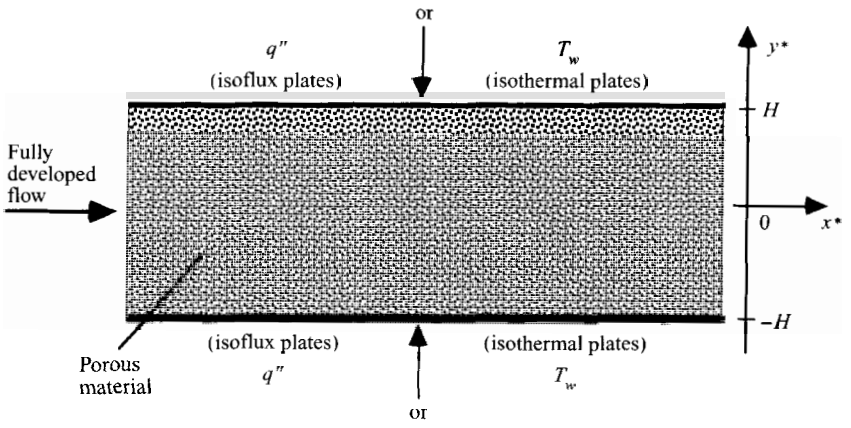

FIGURE 1. Schematic of a fluid saturated porous medium channel bounded by two horizontal isoflux or isothermal plates.

The values of b_1 and b_3 are found in terms of b_2 from the equations $b_1+b_2+b_3=-3/(2FDa)$, and $b_2b_3+b_3b_1+b_1b_2=-3/F$. Hence,

$$(b_1, b_3) = \tfrac{1}{4}F^{-1}\{-3/Da-2Fb_2\pm[9/Da^2+48F-12Fb_2/Da-12F^2b_2^2]^{1/2}\}. \tag{9}$$

Using again the fact that $b_2 = u(0)$, we can integrate (8) to obtain

$$(2F/3M)^{1/2} = \int_0^{b_2}[P(t)]^{-1/2}\,\mathrm{d}t. \tag{10}$$

In a similar fashion, using the boundary condition (3), we obtain

$$(2F/3M)^{1/2}\,y = \int_u^{b_2}[P(t)]^{-1/2}\,\mathrm{d}t. \tag{11a}$$

The integrals in (10) and (11*a*) can be expressed in terms of standard elliptic integrals, $f(\phi\backslash\alpha)$, with the aid of formula 17.4.63 of Abramowitz & Stegun (1965). For example, equation (11*a*) can be written as

$$(2F/3M)^{1/2}\,y = (b_1-b_3)^{-1}f(\phi\backslash\alpha), \tag{11b}$$

where

$$\sin^2\alpha = \frac{b_2-b_3}{b_1-b_3}, \quad \cos^2\phi = \frac{(b_1-b_2)(u-b_3)}{(b_2-b_3)(b_1-u)}. \tag{11c}$$

We may now use the values of $f(\phi\backslash\alpha)$ in table 17.5 of that book, but it is more convenient to evaluate the integrals directly by numerical quadrature. We emphasize that this evaluation can be made as precise as we wish by suitable choice of integration step-size since the only error is that due to round-off. The 'exactness' of our solution and its usefulness for benchmarking are not affected. The amount of computational effort is virtually negligible (at least two orders of magnitude less) in comparison with that involved in numerical integration of the full partial differential equations. Given the values of Da, F and M, the value of b_2 is given in an inverse fashion by (10). Pairs of values (y, u) determining the velocity profile can then be obtained from (11).

With the velocity distribution found, we can now find the temperature distribution.

Following the exposition of Bejan (1984, pp. 82–89), we define a mean velocity U and temperature T_m by

$$U = \frac{1}{H}\int_0^H u^* \,\mathrm{d}y^*, \tag{12}$$

$$T_m = \frac{1}{HU}\int_0^H u^* T^* \,\mathrm{d}y^*, \tag{13}$$

and the Nusselt number Nu by

$$Nu = 2Hq''/k(T_w - T_m), \tag{14}$$

where T_w is the temperature at the wall ($y = 1$). It is worth noting that Vafai & Kim (1989) used a Nusselt number (which we denote by Nu_h) based on the hydraulic diameter, which here is $4H$, i.e. twice the distance between the plates. Hence $Nu_h = 2Nu$.

It follows from the first law of thermodynamics that

$$\partial T^*/\partial x^* = \kappa_m q''/(kHU). \tag{15}$$

We now define a non-dimensional temperature $\hat{T}$ and a new non-dimensional velocity $\hat{u}$ by

$$\hat{T} = (T^* - T_w)/(T_m - T_w), \quad \hat{u} = u^*/U. \tag{16}$$

Notice that this new non-dimensional velocity used in the energy equation, $\hat{u}$, is related with the non-dimensional velocity used in the momentum equation, u, by $\hat{u}(y) = u(y)/\int_0^1 u(y)\,\mathrm{d}y$. Equation (2) now takes the form

$$\frac{\mathrm{d}^2 \hat{T}}{\mathrm{d}y^2} = -\tfrac{1}{2}Nu\,\hat{u}. \tag{17}$$

This must be solved subject to the boundary conditions

$$\hat{T}(1) = 0, \quad \frac{\mathrm{d}\hat{T}}{\mathrm{d}y}(0) = 0. \tag{18}$$

The solution is

$$\hat{T} = \tfrac{1}{2}Nu \int_y^1 \int_0^\eta \hat{u}(\xi)\,\mathrm{d}\xi\,\mathrm{d}\eta. \tag{19}$$

Finally, the Nusselt number Nu can be found by substituting for $\hat{u}$ and $\hat{T}$ in the compatibility condition

$$\int_0^1 \hat{u}\hat{T}\,\mathrm{d}y = 1. \tag{20}$$

We solved the integrals in (10) and (11*a*) using Romberg's numerical integration method (Stoer & Bulirsch 1980), on a semi-open interval (these are improper integrals since the integrands are singular at $u = b_2$), with extended midpoint rule. For simple cases, we checked the results obtained with Romberg's method against results obtained with the more robust (and less efficient) Simpson's fourth-order open formula. We applied the latter method for solving the integrals appearing in (19) and (20).

As a check on our procedure, we recover the known analytical solution for the case $F = 0$. As $F \to 0$, we have, from (9), $b_1 \to (2Da - b_2)$ and $b_3 \to (-\frac{3}{2}F^{-1}Da^{-1})$. Then an asymptotic expansion, valid as $F \to 0$, of the right-hand side of (10) leads to: $\Delta = Da\,\mathrm{sech}\,(\lambda)$, where: $\lambda = (MDa)^{-1/2}$, and $\Delta = (Da - b_2)$. Note that the substitution:

$w = (Da - t)/\Delta$, facilitates the integration. Likewise, (11) gives: $u = Da - \Delta\cosh(\lambda y)$. Hence, we obtain

$$u = Da\left\{1 - \frac{\cosh(\lambda y)}{\cosh(\lambda)}\right\}. \tag{21}$$

This agrees with the expression for the velocity distribution obtained by Kaviany (1985). The solution, equation 8 of Vafai & Kim (1989), fails a similar check. It leads to the prediction that the mid-line velocity differs from the correct value as the Forchheimer parameter tends to zero; the discrepancy is of order $\exp(-Da^{-1/2})$, and this is significant when Da is of order 0.1 or larger. In terms of dimensional quantities, (21) is equivalent to

$$u^* = \frac{GK}{\mu}\left\{1 - \frac{\cosh[(\mu/\tilde{\mu}K)^{1/2} y^*]}{\cosh[(\mu/\tilde{\mu}K)^{1/2} H]}\right\}. \tag{22}$$

We proceed with further checks of our solution. As $Da \to \infty$, (21) gives $u \to (1 - y^2)/2M$, implying that $u^* \to (G/2\tilde{\mu})(H^2 - y^2)$, as expected for plane Poiseuille flow for a fluid clear of solid material. Further, $\hat{u} \to \frac{3}{2}(1 - y^2)$, and so, by (19), $\hat{T} \to \frac{1}{16}Nu(5 - 6y^2 + y^4)$, and, by (20), $Nu \to \frac{70}{17}$, or approximately 4.1176. This agrees with the well-known value of Nu for the clear-fluid problem.

As $Da \to 0$, equation (21) gives $u \to Da$, (if $|y| \neq 1$), implying that $u^* \to KG/\mu$, as expected for Darcy flow. Further, $\hat{u} \to 1$, and so, by (19), $\hat{T} \to \frac{1}{4}Nu(1 - y^2)$, and, by equation (20), $Nu \to 6$. The final result agrees with equation (4.40) of Nield & Bejan (1992).

For a general value of Da (but still with $F \to 0$) we find that in the limit,

$$\hat{T} = \frac{Nu}{4\lambda(\lambda - \tanh\lambda)}\left\{\lambda^2(1 - y^2) + 2\left[\frac{\cosh\lambda y}{\cosh\lambda} - 1\right]\right\}, \tag{23}$$

and this leads to

$$Nu = \frac{12\lambda(\lambda - \tanh\lambda)^2}{2\lambda^3 + 3\lambda\tanh^2\lambda + 15(\tanh\lambda - \lambda)}. \tag{24}$$

Eliminating Nu from these two equations yields

$$\hat{T} = \frac{3\lambda(\lambda - \tanh\lambda)}{2\lambda^3 + 3\lambda\tanh^2\lambda + 15(\tanh\lambda - \lambda)}\left\{\lambda^2(1 - y^2) + 2\left[\frac{\cosh\lambda y}{\cosh\lambda} - 1\right]\right\}. \tag{25a}$$

These formulae are in agreement with those obtained by Lauriat & Vafai (1991, p. 312). However, they wrote, 'These analytical results are in agreement with the numerically obtained results of Kaviany (1985) for laminar flow through a porous channel bounded by isothermal plates', and they went on writing that Nu_h (which equals $2Nu$) varied between the asymptotic values 7.54 (for Newtonian fluid flow) and 9.87 (for Darcian flow). In fact, Nu as given by (24) varies from 4.12 ($\lambda \to 0$, i.e. for Newtonian fluid flow) to 6 (for $\lambda \to \infty$, i.e. for Darcian flow), as we would expect. We emphasize that (24) and (25a) apply only to the case of constant-flux boundaries. These formulae have been obtained on the assumption that $\partial T^*/\partial x^*$ is independent of y^*. Equivalent formulae had already been derived, in the correct context, by Nakayama *et al.* (1988).

It is clear that as Da tends to zero the differential equation system becomes singular. In this case the Brinkman term is negligible and the velocity profile is flat (slug flow). The velocity u is given by the appropriate root of the equation

$$FDa\,u^2 + u - Da = 0, \tag{25b}$$

namely

$$u = \{-1+(1+4FDa^2)^{1/2}\}/2FDa. \tag{26}$$

In this case we have, for all values of F,

$$\hat{u} = 1, \quad \hat{T} = \tfrac{3}{2}(1-y^2), \quad Nu = 6. \tag{27a}$$

The same situation arises as F tends to infinity.

3. Isothermal surfaces: theory

As explained by Bejan (1984, pp. 89–90), consideration of the first law of thermodynamics shows that the mean temperature difference must decrease exponentially in the flow direction, x (see figure 1):

$$T_w - T_m = (T_w - T_1)\exp[-\kappa_m Nu'(x^* - x_1)/2H^2U], \tag{27b}$$

if $T_m = T_1$ at $x^* = x_1$, where Nu' is the Nusselt number for isothermal boundaries. Consequently equation (2) now leads to

$$\frac{\mathrm{d}^2\hat{T}}{\mathrm{d}y^2} = -\tfrac{1}{2}Nu'\,\hat{u}\hat{T}. \tag{28}$$

This holds in place of (17). The boundary conditions, equation (18), still hold. In place of (20), the compatibility condition is

$$Nu' = -2\frac{\mathrm{d}\hat{T}}{\mathrm{d}y}\bigg|_{y=1}. \tag{29}$$

The velocity $\hat{u}(y)$ is unchanged, but now we have a two-point boundary-value problem constituted by equations (28), (18) and (29). The solution of this problem, for general parameters, is obtained numerically. Equation (28) is discretized in y using a second-order finite-differences scheme. We emphasize that once the exact velocity profile has been obtained, it is a relatively easy numerical task to obtain the temperature field for any choice of thermal boundary conditions. For every (Da, F, M) group, the corresponding velocity profile, obtained previously, is used in (28). Notice that for the isothermal case, the two boundary conditions in (18) lead to the trivial solution $\hat{T} = 0$. This is avoided by writing an expression for the temperature at the first interior node near the surfaces as a function of Nu', via a discretized compatibility condition. The problem is now restricted to finding the Nu' value that best satisfies the temperature condition imposed at $y = 1$. We note in passing that a shooting method, as suggested by Bejan (1984), is also possible although not so straightforward. Some theoretical solutions for extreme flow cases are now described. For the particular case $F = 0$, $Da \to 0$, the solution is: $\hat{T} = \frac{1}{2}\pi\cos\frac{1}{2}\pi y$, $Nu' = \frac{1}{2}\pi^2 \sim 4.93$. For $F = 0$, $Da \to \infty$, the value of Nu' is 3.77 (see for instance table 3.2 of Bejan 1984). These results were used to verify the accuracy of our finite-differences scheme.

4. Isoflux surfaces: numerical results and discussion

For general values of F and Da numerical calculation is necessary. In general, the numerical quadrature is straightforward, but, as noted above, b_2 has to be found from (10) in an inverse fashion. As one would expect, there are severe numerical difficulties as one approaches a parameter value for which the system is singular. In the case of

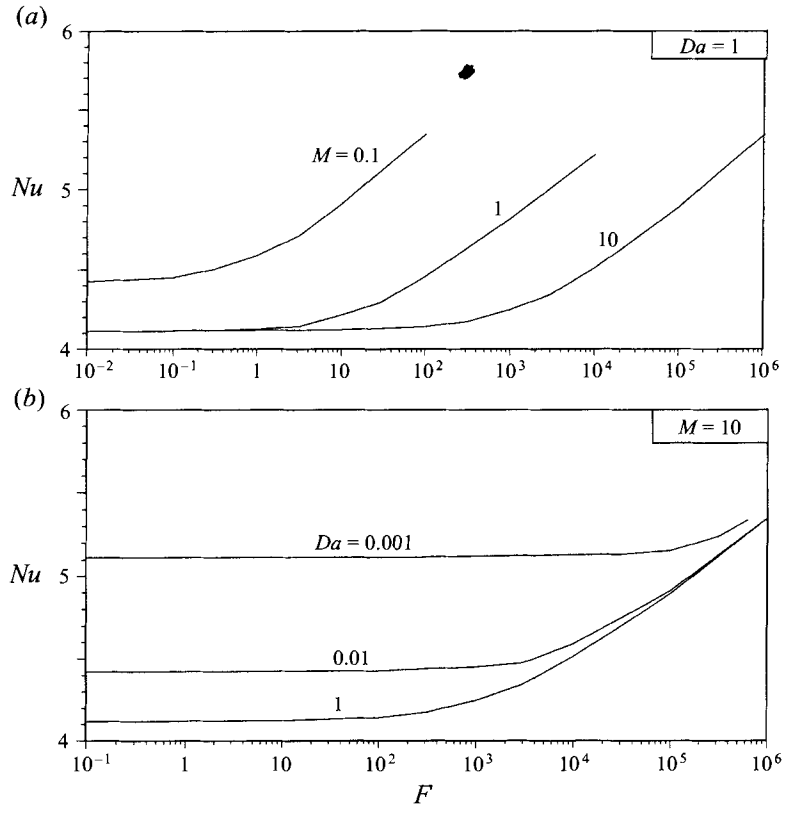

FIGURE 2. Effect of Forchheimer number, F, on the Nusselt number, Nu for isoflux surface case.

large F, these are associated with the fact that the roots b_2 and b_3 coalesce in the limit. It is fortunate that, because the asymptotic results are available, we need not persist with the difficult calculations.

The results of our calculations for representative values of the parameters are displayed in figures 2–5. The trends shown are in conformity with our expectations. Figure 2(*a*) gives values of the Nusselt number, Nu, for Darcy number equal to 1, a rather large value. As the Forchheimer number F tends to zero, each curve approaches a horizontal asymptote. The asymptotic values of Nu are 4.431, 4.159, 4.122, for $M = 0.1$, 1, 10, respectively, in agreement with (24) with $\lambda = 10^{1/2}$, 1, $10^{-1/2}$, respectively. As F becomes large, the value 6 is approached. The approach is slow for large values of M. The effect of increasing the quadratic drag is to increase the Nusselt number, the effect of a given amount of quadratic drag being less dramatic if M is large. We note here that although at first sight it might be considered as an unrealistically high value, the case of $M = 10$ is well in line with the experimental results obtained very recently by Givler & Altobelli (1994) for the viscosity ratio for flow through high-porosity media.

The effect of Nu of varying Da, with M fixed at 10, is shown in the lower part of figure 2. For small values of F, the values of Nu again agree with (24), the asymptotic values for $Da = 0.001$, 0.01, 1 being 5.129, 4.431, 4.122, respectively. In accordance with the above asymptotic result, Nu tends to the 'slug flow' value 6 when F becomes large, no matter what the value of Da is.

The way in which the velocity and temperature profiles change with Da, F, and M

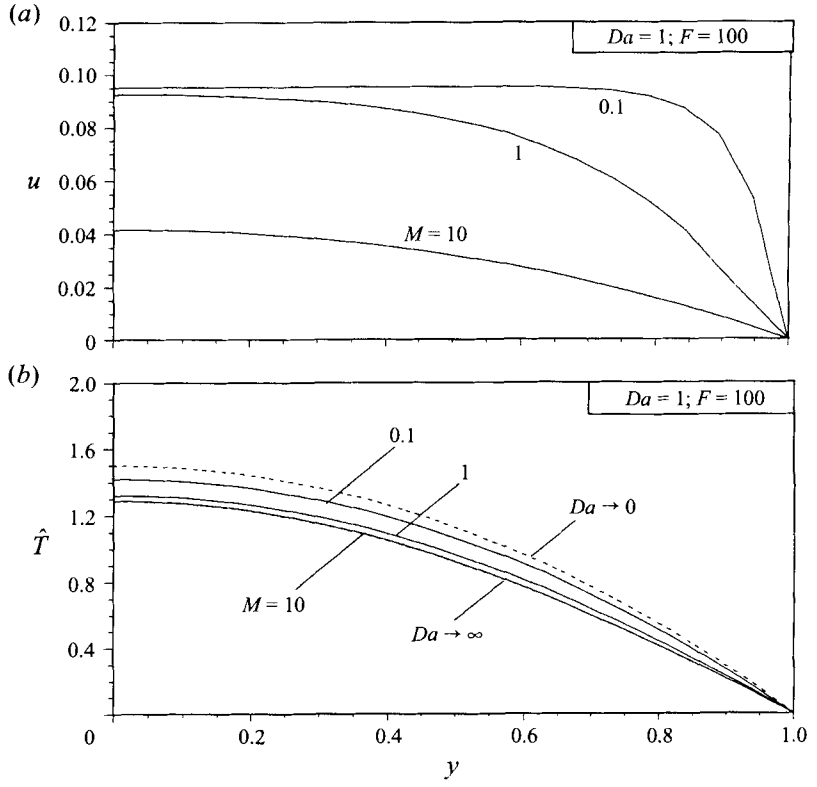

FIGURE 3. Viscosity ratio, M, effect on (a) velocity u and (b) temperature $\hat{T}$ half-channel profiles for the isoflux surface case.

is shown in figures 3, 4 and 5 for isoflux surfaces. Figure 3 is for fixed Forchheimer number, $F = 100$, and for fixed Darcy number, $Da = 1$, though for ease of comparison the asymptotic temperature profiles for $Da \to 0$ and for $Da \to \infty$ are also displayed. Variation of M has a dramatic effect of the velocity profile but considerably less effect on the temperature profile. It follows from (7) that $(MDa)^{1/2}$ is a measure of the thickness of the momentum boundary layer, and the calculated results agree with that fact. There is no similar thermal boundary layer for the present situation.

The effect of varying F, for fixed values of Da and M, is shown in figure 4. The way in which the velocity profile is flattened as F increases is clearly shown. This, of course, lies behind the increase of the Nusselt number which we noted when discussing figure 2. Simultaneously, the mean value of our non-dimensional velocity is substantially reduced. This is as expected, because the physical velocity has been scaled using a quantity proportional to the applied pressure gradient, and for large F the physical velocity must be approximately proportional to the square root of the pressure gradient. Again, the temperature profile is not greatly altered as F increases, but there is a convergence towards the parabolic profile given by (27).

Finally, in figure 5 we see the effect of varying Da, with M and F held constant. The velocity profile becomes flatter, and the mean non-dimensional velocity becomes smaller, as Da becomes smaller. This is as expected, since small Da corresponds to relatively small permeability, and hence to less flow for a given pressure gradient. Simultaneously, the effect of the Brinkman term is confined to a thinner boundary

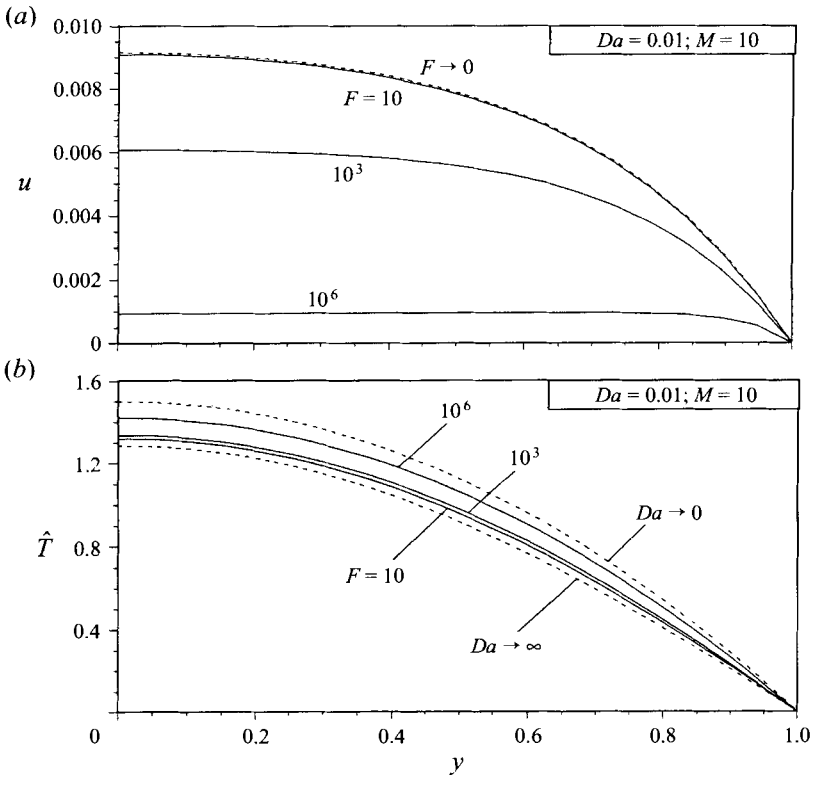

FIGURE 4. Forchheimer number, F, effect on (*a*) velocity u and (*b*) temperature $\hat{T}$ half-channel profiles for the isoflux surface case.

layer. The change in the temperature profile is also as expected. Again the parabolic profile is approached as $Da \to 0$.

Vafai & Kim (1989, p. 1106) wrote that 'the Nusselt number increases with an increase in the inertia parameter. This is because an increase in the inertia parameter, due to a more vigorous mixing of the fluid, causes a more uniform velocity profile.' It is true that hydrodynamic dispersion increases as the flow velocity increases, but there is no major change here analogous to that which occurs when there is a transition from laminar to turbulent flow in a clear fluid. Rather, a basic feature of channel flow in a dense porous medium is the tendency for the flow to be uniform except in a boundary layer adjacent to the wall. As the velocity increases, the total Darcy–Forchheimer drag increases in the bulk of the medium. Near the wall, this must be balanced by an increased frictional drag, and this requires a greater shear. This implies that a thinner boundary layer must be present for high-speed flow.

It is interesting to explain why there is a significant increase in the Nusselt number for a relatively high-permeability medium as the inertia parameter increases. One cannot explain this by a flattening of the temperature profile. Our results (and those obtained by Vafai & Kim, 1989) show that the increase in F can cause the Nusselt number to increase by an amount as large as 50%. The maximum change in the shape of the temperature distribution is less than 20% and, in any case, an increase in F causes a sharpening, not a flattening, of the temperature profile, as shown by our figure 4. The important thing is the way in which the mean temperature is defined (see (13)). The temperature is weighted by the velocity. When one has slug flow, T_m is just the

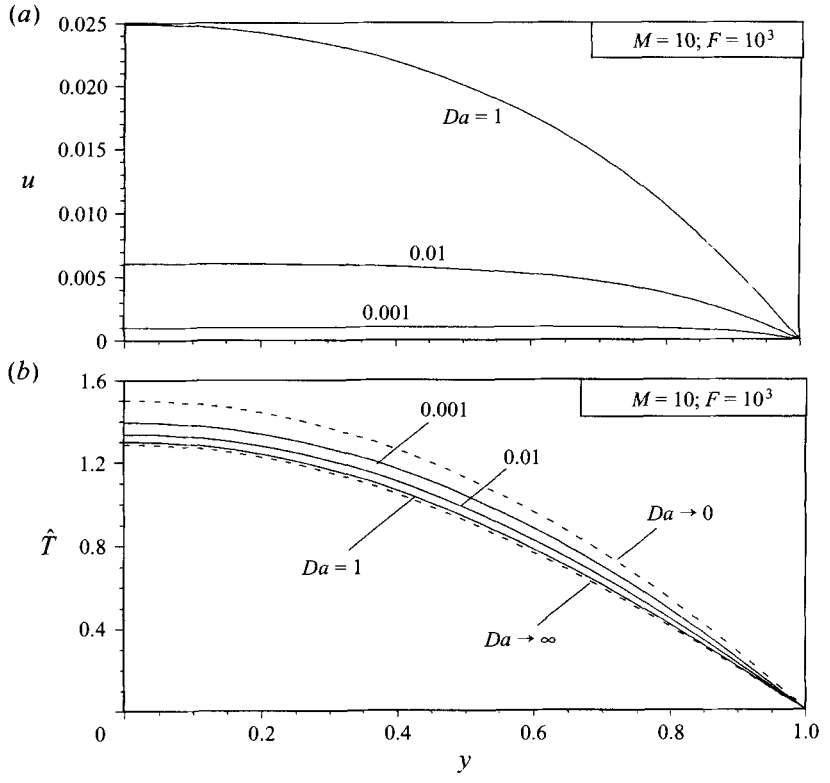

FIGURE 5. Darcy number, *Da*, effect on (*a*) velocity u and (*b*) temperature $\hat{T}$ half-channel profiles for the isoflux surface case.

ordinary average temperature. When one has a velocity profile with less flow near the walls than in mid-channel (as in the case of the parabolic profile), the portion further from the walls is weighted higher than that near the walls. Since the temperature decreases monotonically away from the walls, the effect of this differential weighting is to increase $(T_w - T_m)$. The effect of an increase in F is to produce a more slug-like flow, and this directly decreases $(T_w - T_m)$, and this leads, via the factor $(T_w - T_m)^{-1}$ in the definition of Nu (equation (14)), to an increase in Nu.

5. Isothermal surfaces: numerical results and discussion

Figure 6(*a*) shows the Nusselt number and figure 6(*b*) the temperature distribution for isothermal surfaces. The isothermal case Nusselt number is slightly smaller than for constant-flux boundaries, and we would expect this trend to continue for general values of F and Da. The Nusselt number is smaller because the temperature difference $(T_m - T_w)$ is larger, because in turn the temperature profile is more peaked, because the extra factor $\hat{T}$ in the right-hand side of (26) (cf. (17)) means that the curvature of the profile is greater in the centre of the channel than near the walls, because the convective heat transfer is greater in the centre of the channel than nearer the walls in the case of constant-temperature boundaries (rather than constant as in the case of constant-flux boundaries), because the axial component of the temperature gradient increases with distance from the wall (rather than being constant), because of the first law of thermodynamics.

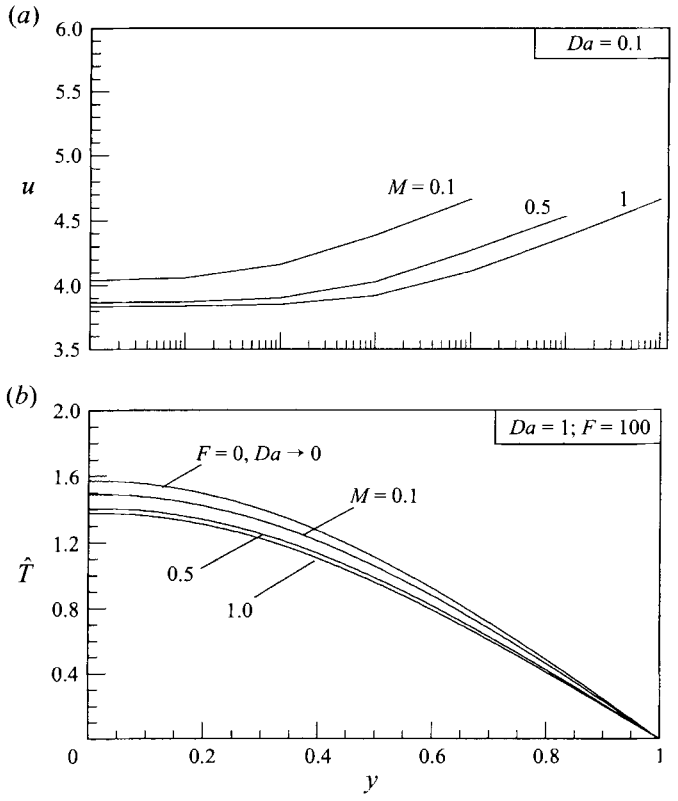

FIGURE 6. (*a*) Nusselt number and (*b*) temperature for isothermal surfaces case.

The effect of changes in the values of the parameters M, Da and F appears to be primarily a consequence of changes of the velocity profile, while the change from constant flux to constant temperature is clearly a thermal effect. It is plausible that these two effects might be only loosely coupled. This suggested to us that a reasonable estimate of Nu' might be obtained from our calculated results for constant flux boundaries by introducing a new linear ordinal scale in figure 2, with the mark $Nu = 4.12$ replaced by $Nu' = 3.77$ and with the mark $Nu = 6.00$ replaced by $Nu' = 4.93$. This is equivalent to making the transformation

$$Nu' = 3.77 + 0.617\,(Nu - 4.12). \tag{30}$$

The computed values of Nu' presented in figure 6 are in fact in approximate accord with this relationship.

6. Conclusions

We have performed a fresh theoretical analysis of fully developed forced convection in a fluid-saturated porous-medium channel bounded by parallel plates. Our general solution, with no restrictions, extends existing solutions to all values of the Darcy number and Forchheimer inertia coefficient. It also applies to a medium with effective viscosity different from the fluid viscosity. The result is an efficient and broad tool for predicting transport phenomena even within high-permeability media. For the isoflux case, the solution is accurate to the extent that it predicts exactly the flow and thermal characteristics of known asymptotic regimes.

With the aid of our theoretical solution of the Brinkman–Forchheimer extension of Darcy's equation, we have elucidated the effects of quadratic drag and boundary friction on fully developed forced convection in a saturated porous medium confined between isoflux or isothermal parallel plates. For each type of boundary, the temperature profile is little changed as a result of variation of the viscosity ratio, Darcy number or Forchheimer number. It is slightly more peaked when Da is small or when F is large, and especially so when M is small. On the other hand, the Nusselt number is significantly altered, primarily as a direct consequence of the change in velocity profile.

In particular, for the case of isoflux surfaces, the following holds. When simultaneously Da is large and F is small, the velocity profile is approximately parabolic and the Nusselt number is near 70/17 (a lower bound). When either Da is sufficiently small or F is sufficiently large (the criterion being quickly reached when M is relatively small), the velocity profile is approximately uniform (apart from a thin boundary layer) and the Nusselt number is near 6 (an upper bound). For the case of isothermal surfaces the story is similar, but the Nusselt numbers are smaller. The sets of Nusselt numbers for the two cases are related approximately by (30).

We also note that the numerical results of Kaviany (1985) show that the velocity field generally develops to its steady-state form in a short distance from the entrance, of order $(K\bar{u}/\nu)$, where $\bar{u}$ is the entrance velocity (the same was also predicted by Vafai & Kim (1981), for flow over a plate in a saturated porous medium). The exception is when $Da > 1$. For this case, a fully-numerical approach is probably the best method of investigation. The problem of thermal development is of more immediate interest. Now that we have the velocity distribution in closed form, a series solution of the Graetz type is a viable alternative to a fully-numerical solution.

J.L.L. acknowledges with gratitude the support provided by Southern Methodist University through the J. L. Embrey Professorship in Mechanical Engineering. S.L.M.J. is thankful for the financial support from CNPq, the Brazilian National Research Council. The authors are indebted to Professor Vafai for providing additional information, which has shown that some aspects of our earlier assessment (in drafts of the present paper) of Vafai & Kim (1989) were erroneous, and we apologize to Professor Vafai and Dr Kim for this.

Note added in proof. Professor P. Cheng has drawn our attention to Cheng, Hsu & Chowdhury (1988). In this paper an analytical solution for the velocity, which is based on a boundary layer approximation and so is valid for small Da only, and which is essentially the same as that given by Vafai & Kim (1989) and is related to the asymptotic solution given by Vafai & Thiyagaraja (1987), is presented.

REFERENCES

ABRAMOWITZ, M. & STEGUN, I. A. (ed.) 1965 *Handbook of Mathematical Functions*. Dover.

BEJAN, A. 1984 *Convective Heat Transfer*. Wiley.

CHENG, P., HSU, C. T. & CHOWDHURY, A. 1988 Forced convection in the entrance region of a packed channel with asymmetrical heating. *Trans. ASME* C: *J. Heat Transfer* **110**, 946–954.

GIVLER, R. C. & ALTOBELLI, S. A. 1994 A determination of the effective viscosity for the Brinkman–Forchheimer flow model. *J. Fluid Mech.* **258**, 355–370.

KAVIANY, M. 1985 Laminar flow through a porous channel bounded by isothermal parallel plates. *Intl J. Heat Mass Transfer* **28**, 851–858.

LAGE, J. L., PRICE, D. C., WEBER, R. M., SCHWARTZ, G. J. & MCDANIEL, J. 1996 Improved cold

plate design for thermal management of phased array radar systems. *US Patent Office*, patent pending.

LAURIAT, G. & VAFAI, K. 1991 Forced convective flow and heat transfer through a porous medium exposed to a flat plate or a channel. *Convective Heat and Mass Transfer in Porous Media* (ed. S. Kakaç, B. Kilkiş, F. A. Kulaki & F. Arinç), pp. 289–327. Kluwer.

NAKAYAMA, A., KOYAMA H. & KUWAHARA, F. 1988 An analysis on forced convection in a channel filled with a Brinkman–Darcy porous medium: exact and approximate solutions. *Wärme- und Stoffübertragung* **23**, 291–295.

NIELD, D. A. & BEJAN, A. 1992 *Convection in Porous Media*. Springer.

POULIKAKOS, D. & RENKEN, K. 1987 Forced convection in a channel filled with porous medium, including the effects of flow inertia, variable porosity, and Brinkman friction. *Trans. ASME* C: *J. Heat Transfer* **109**, 880–888.

RAJASUBRAMANIAN, G., MEIDELL, R. S., LANDAU, C., DOLLAR, M. L., HOLT, D. B., WILLARD, J. E., PRAGER, M. D. & EBERHART, R. C. 1994 Fabrication of resorbable microporous intravascular stents for gene therapy applications. *ASAIO J.* **40**, M584–589.

RENKEN, K. & POULIKAKOS, D. 1988 Experiment and analysis of forced convective heat transport in a packed bed of spheres. *Intl J. Heat Mass Transfer* **31**, 1399–1408.

STOER, J. & BULIRSCH, R. 1980 *Introduction to Numerical Analysis*. Springer.

VAFAI, K. & KIM, S. J. 1989 Forced convection in a channel filled with a porous medium: an exact solution. *Trans. ASME* C: *J. Heat Transfer* **111**, 1103–1106.

VAFAI, K. & KIM, S. J. 1995 Discussion of 'Forced convection in a porous channel with localized sources'. *Trans. ASME* C: *J. Heat Transfer* **117**, 1097–1098.

VAFAI, K. & THIYAGARAJA, R. 1987 Analysis of flow and heat transfer at the interface region of a porous medium. *Intl J. Heat Mass Transfer* **30**, 1391–1405.

VAFAI, K. & TIEN, C. L. 1981 Boundary and inertia effects on flow and heat transfer in porous media. *Intl J. Heat Mass Transfer* **24**, 195–203.

WEINERT, A. & LAGE, J. L. 1994 Porous aluminum-alloy based cooling devices for electronics. *SMU-MED-CPMA Inter. Rep.* 1.01/94.